Semnan University

Journal of Heat and Mass Transfer Research

Journal homepage: https://jhmtr.semnan.ac.ir

ISSN: 2383-3068

Research Article

Effects of Uniform Injection and Suction on the Flow of a Rivlin-Ericksen Fluid of Grade Three through Porous Parallel Plates: A Semi-Analytical Study

Deepika Priyadarsini Palai [a], Sumanta Chaudhuri [b]*, Bitanjaya Das [a]

[a] School of Civil Engineering, Kalinga Institute of Industrial Technology, Deemed to be University, Bhubaneswar, Pin, Odisha,751024, India

[b] School of Mechanical Engineering, Kalinga Institute of Industrial Technology, Deemed to be University, Pin, Odisha,751024, India

ARTICLE INFO

Article history:

Received: 2023-11-05

Revised: 2024-06-10

Accepted: 2024-07-23

Keywords:

Least square method;

Rivlin-Ericksen fluids;

Perturbation method;

Uniform suction/injection;

Porous plate.

ABSTRACT

Numerous industrial and biological processes like water filtering, air filtering, blood flow through arteries, and absorption of digested foods are a few examples of flow with suction/injection at the walls. Studies related to the injection/suction of Newtonian fluids have been reported by several researchers in the past, but studies related to the flow of non-Newtonian fluids with injection/suction are scarce in the open literature. Rivlin-Eriksen fluid (also known as third-grade fluids) is an important class of non-Newtonian fluids that is applied for modeling crude and slurry material in a liquid state, molten lava, blood flow, petroleum etc. Considering this, the flow of a Rivlin-Ericksen fluid of grade three through large porous parallel plates with bottom injection and top suction (same velocity of suction and injection) is analyzed in the present study. The governing equations of fluid flow are solved by using the least square method, which is an important part of the present study. Choosing the trial function for the least square method in this particular case is a difficult task since the velocity profile turns out to be asymmetric for higher velocity of suction and injection. In this study, proper implementation of the least square method is demonstrated for such types of asymmetric velocity distribution, which is a novelty. In the present study a solution for non-dimensional velocity distribution is obtained, and the results are validated with the solution obtained by perturbation method. The results reveal that with an increase in the non-Newtonian parameter (when the cross-flow Reynolds number is low), velocity decreases at the same rate, both near the bottom and top walls. However, when the cross-flow Reynolds number is higher, velocity near the bottom plate is nearly unaffected by a decrease in the non-Newtonian parameter, whereas, near the top plate, velocity decreases with an increase in the non-Newtonian parameter.

1. Introduction

In mass transfer, cooling, suction or injection (blowing) through boundaries can play a crucial role by significantly affecting velocity profiles. As a consequence, heat transfer to or from surfaces is also affected appreciably. Injection and suction through porous walls are of immense practical importance due to their application of boundary layer control in wire coating, film cooling and polymer fiber coating [1].

* **Corresponding author.**
E-mail address: *sumanta.chaudhurifme@kiit.ac.in*

Cite this article as:

Palai, D. P., Chaudhuri, S. and Das, B., 2025. Effects of Uniform Injection and Suction on the Flow of a Rivlin-Ericksen Fluid of Grade Three through Porous Parallel Plates: A Semi-Analytical Study. *Journal of Heat and Mass Transfer Research*, 12(1), pp. 45-60.

https://doi.org/10.22075/JHMTR.2024.32255.1496

The effect of suction is to enhance heat transfer rate and to increase skin friction, whereas the effect of the injection is just the opposite. During emergency shutdowns in nuclear reactors, slot suction/injection can serve to be very effective [2]. In view of this, numerous researchers studied the impact of injection/suction on flow and heat transfer behavior over slender cylinders. Ishak et al. [1] examined the effect of uniform suction/injection on the flow and heat transfer characteristics over a cylinder in stretching condition. The partial differential equations, using a set of similarity transformations, were converted to a set of ordinary differential equations and a numerical solution was obtained. The impact of the suction/injection parameter, Reynolds number, and Prandtl number on the velocity, temperature, Nusselt number and skin friction coefficient were analyzed. The results revealed that temperature was reduced for both air (Prandtl number 0.7) and water (Prandtl number 7) with an increase in the suction/injection parameter. In the study of Datta et al. [2], effect of slot injection/suction on flow over a slender cylinder, with the formation of a boundary layer, was studied, and the governing dimensionless equations were solved numerically. Effects of viscous dissipation, curvature, and Prandtl number on velocity, temperature and skin friction were discussed. Researchers also studied magnetohydrodynamic (MHD) transport and heat transfer in nano fluids through parallel plates with injection/suction. Heat transfer in Al_2O_3-Cu/Water micropolar, hybrid nano fluid flowing through a channel with a permeable wall, including chemical reaction and magnetic field, was examined by Mollamahdi et al. [3]. The lower wall was considered to be hot, and the cold fluid was injected from the top. The governing equations were solved by the least square method (LSM), and the effects of Reynolds number, Hartmann number, micro rotation factor, concentration of nano particles on the velocity and heat transfer were examined. Results indicated that the temperature reduced and concentration increased with an increase in Hartmann number. The studies cited in the preceding discussion considered flow through porous boundaries only. Flow and heat transfer of fluids through porous bounding surfaces of porous media is also an important research area as it finds wide applications in the fields of biomedical, chemical, filtration, solar heat exchangers, ground water movement etc. Even the desalination process [4] is affected by the porosity of the nano sheet [5]. The case of combined conduction-convection-radiation heat transfer, arising in the field of solar heat exchangers filled with fluid saturated cellular porous medium, was examined by Deghan et al. [6]. The flow was modeled by the Darcy-Brinkman equation, and the Homotopy perturbation method (HPM) was applied to obtain a semi-analytical solution, and a numerical solution was obtained by the finite difference method. The influence of porous medium shape number and radiation parameter on thermal performance were discussed. The influence of uniform suction/injection on drag coefficient and turbulence characteristics at moderate Reynolds number up to 2500 was considered by Kametani et al. [7]. Results revealed that 10% drag reduction and enhancement were achieved by injection and suction, respectively. Unsteady MHD convection through a loosely packed permeable media into a precipitately started perpendicular plate was studied by Chandrasekhar et al. [8]. Velocity was observed to decrease with an increase in magnetic field. The Stagnation-point flow of a Walters' B fluid towards a vertical stretching surface, which was embedded in a porous medium, with chemical reaction and deformation, was studied by Akinbo and Olajuwon [9]. Governing partial differential equations were converted to ordinary differential equations by similarity transformation, and an analytical solution was obtained. Chemical reaction and radiation effects on unsteady coupled heat and mass transfer in natural convection from a vertical plate embedded in a porous medium were studied by Aly et al. [10]. The governing equations were solved numerically by the finite difference method, and the effects of relevant parameters on velocity, temperature and Nusselt number were examined. Umavathi et al. [11] investigated oscillatory, unsteady heat transfer and flow in a horizontal channel filled with composite substances. The Darcy-Brinkman equation was applied to model the flow. Partial differential equations were solved, and analytical solutions were obtained utilizing functions that were harmonic and non-harmonic. The influence of porous medium parameter, viscosity ratio, Prandtl number, and oscillation amplitude were analyzed. Velocity and temperature were reduced with an increase in porous parameter. It was found that when the porous parameter increased from 1 to 2, the maximum velocity reduced from nearly 1.8 to 1.3. Thermally developing forced convective heat transport in a channel filled with porous material was examined by Deghan et al. [12]. The channel walls were subjected to uniform heat flux. The two-energy equation model, along with Darcy's law of motion, were considered. Nusselt number for thermally developing condition in a porous material for LTNE (local thermal non

equilibrium) and the developing length was predicted. The impact of variable thermal conductivity on forced convective heat transfer through a parallel-plate heat exchanger filled with porous medium was studied by Deghan et al. [13]. The channel walls were subjected to uniform and constant heat flux and the governing equations were analytically solved using the perturbation method. Expressions for Nusselt number and temperature distribution were deduced in terms of porous parameter and thermal conductivity variation parameter. Deghan et al. [14] also studied conjugate heat transfer in microchannels filled with porous medium. The effect of slip and internal heat generation were considered. Analytical solution was obtained for local thermal non-equilibrium condition, and the effect of dimensionless wall resistance, Bio number, heat generation parameter, fluid to solid effective conductivity ratio on Nusselt number and temperature were examined. Chakravarty et al. [15] studied heat transport in mixed convection, occurring in an enclosed space having a porous bed with heat generating capacity and injection of cold fluid from the bottom of the porous bed. During post accident situations in nuclear reactors, this type of condition occurs when enhancement of heat removal is essential by cold fluid injection from the bottom. In this study, the Darcy-Brinkman-Forchheimer approximation was used for modeling the flow through porous media. Equations governing the physical phenomenon were solved by the computational fluid dynamics software ANSYS FLUENT. It was observed that permeability factor of the flow media significantly affected the flow near the inlet. Heat transport in mixed convection in a porous, square cavity in nano fluids considering injection/suction regions, Brownian diffusion and thermophoresis was investigated by Sheremet et al. [16]. The finite difference method was employed to yield numerical solutions to the equations, and the outcomes were validated with the experimental study. It was reported that an increment in cross-flow Reynolds number (indicating the inlet vertical velocity of nano fluid inside the cavity) causes thinning of the thermal boundary layer near the hot wall.

The above discussion highlighted a few important studies on the influence of injection/suction on flow characteristics and heat transfer characteristics through porous media and through porous boundary with the flow of Newtonian fluids. It is well known that many fluids used in industries fall in the category of non-Newtonian fluids, and heat transport and flow involving various non-Newtonian fluids were analyzed by researchers. Some of the frequently adopted non-Newtonian fluid models are the Power law model [17, 18], the Casson model [19,20], the Visco-elastic model [21-23], Rivlink-Eriksen fluid of grade two [24], three [25-27] (second and third grade fluids). Due to the importance of porous media and porous boundary transport, researchers are actively engaged in the study of different aspects of flow features and heat transport of non-Newtonian fluids in porous media and through porous boundaries. Gupta et al. [17] studied the impact of injection/suction on the flow features and heat transport of a power law fluid over a flat plate. It was reported that steady state solution exists for only shear-thinning fluids for which the power-law index n varies in the range $0 < n < 1$ and suction takes place at the plate. In the case of injection, steady state velocity distribution was not observed to exist. The heat transport of a non-Newtonian power law fluid passing a moving surface was examined by Radnia and Nazar [18], considering uniform injection/suction. The surfaces were assumed to be subjected to uniform wall temperature. The results indicated that the boundary layer thickens with an increase in suction. It also increases with internal heat generation. Thermosolute free convection in isotropic, porous cylindrical cavity, filled with Casson nano fluid, subjected to external magnetic effect was studied by Mustapha et al. [19]. The governing equations were solved numerically by the finite volume method, and the effects of different parameters on heat transfer rate and concentration were analyzed. Mass and heat transfer rates were observed to increase with the rise in the Casson fluid parameter, and this increase is significant when the Casson fluid parameter lies in the range 0.1-0.4. Magnetohydrodynamic flow in Casson fluid with slip condition, with a stretching sheet, under the effect of injection/suction was examined by Madhy [20]. The partial differential equations, describing the flow and heat transfer effect, were reduced to a set of ordinary differential equations by a similarity transformation method and were solved numerically. It was reported that an increment in the Casson parameter suppressed the velocity field. The temperature, on the other hand, increased with an increase in Casson parameter. Dash and Ojha [21] studied MHD flow of a visco-elastic fluid between two porous parallel plates under the action of a pressure gradient which was sinusoidal. Results indicated that an oscillating pressure gradient, with low frequency, prevents the back flow and skin friction was reduced significantly by embedding the channel in porous medium. Electro kinetic transport of visco-elastic and Newtonian fluids in model porous media with

long micro pores was studied by Khan and Sasmal [22]. Numerical solution for both Newtonian and viscoelastic fluids were obtained. Over the entire range of parameters considered in the study, a steady and symmetrical velocity field was observed for Newtonian fluids. For visco-elastic fluids, a transition from symmetric and steady to asymmetric and unsteady profile takes place when the Weissenbarg number crosses a critical limit. Padma Devi and Srinivas [23] considered bi-layered, immiscible flow of a viscoelastic liquid in a porous, vertical channel including the effects of Hall current, chemical reaction and radiation. The pressure gradient was considered as oscillatory. Solutions for concentration, velocity, and temperature were obtained utilizing the perturbation method. For a Newtonian fluid, a symmetric and steady field was observed, whereas for viscoelastic fluids, it was observed that a transition from symmetric and steady flow to an asymmetric and unsteady flow took place when the Weissenberg number crossed a critical limit. Third-grade fluid is another class of non-Newtonian fluids that drew the attention of various researchers. The second, and third fluids come in a subclass of differential type Rivlin-Ericksen fluids. It was reported that blood [25] and scientifically treated petroleum motor oil [26] additives consisting of polyisobutylene polymer, in dissolved condition in petroleum, follow the third-grade fluid model. The third-grade fluids have shear dependent viscosity, but this characteristic is missing in second grade fluids. Due to this shortcoming, second grade fluids are not able to predict shear-thinning and shear-thickening properly. However, second grade fluids can predict the normal stress difference. Flow features and heat transport characteristic of third grade fluids and their different aspects have been studied by researchers [25-28]. Flow features and heat transport aspects of third grade fluids through porous media were considered in those studies. Hayat et al. [27] studied MHD flow of a third-grade fluid in a porous channel. Homotopy analysis method was applied to find the velocity distribution. The entropy generation rate in the MHD flow of a third-grade fluid in parallel plates with porous media was studied by Adesanya and Falade [28]. The flow was actuated by applied constant pressure gradient and influenced by the applied magnetic field. The equations were solved using the perturbation method.

The discussion above establishes the requirement of studies on flow features and heat transfer of third grade fluids in porous media and through porous boundaries. Therefore, in the recent study, the flow of a third-grade fluid in large parallel plates with the effect of uniform injection and suction is considered. This type of study was carried out for the second-grade fluid by Ariel [24]. In the study of Ariel [24], exact solutions for the non-dimensional velocity distribution were obtained for two geometries. One was for flow through large parallel plate and the second was for flow through concentric annular cylinders. For a third-grade fluid flow, in the current study, the least square method (LSM) is applied to find the solution for the non-dimensional velocity field. LSM is a very useful semi-analytical method which was employed by numerous researchers [3, 29] for solving fluid flow and heat transfer problems. In the present study, the non-linear governing differential equations are first reduced to their dimensionless forms, and then solution by the LSM is obtained. Further, a solution by the traditional perturbation method is obtained for small values of the third-grade fluid parameter and cross-flow Reynolds number. These two results are compared for validation purposes, and the results are in excellent agreement. Further, the results of the LSM solution are compared with the outcomes of a Newtonian fluid in the limiting case of vanishing non-Newtonian parameter. It is observed that the LSM results are in exact match with that of the Newtonian solution. These two comparisons serve the purpose of validation of the results obtained in the present study. Then, the impact of cross-flow Reynolds number and third-grade fluid parameter on the dimensionless velocity are analyzed. To highlight the novelties of the present study, a brief review of the previous studies on non-Newtonian fluids in this field is presented in Table 1.

Table 1. Studies on porous media and porous boundary flow with suction/injection in non-Newtonian fluids

References	Content
Padma Devi and Srinivas (2023)	Authors considered bi-layered, immiscible flow of a viscoelastic liquid in a porous, vertical channel, including the effects of Hall current, chemical reaction and radiation. The pressure gradient was considered as oscillatory. Solutions for concentration, velocity, and temperature were obtained utilizing the perturbation method. For a Newtonian fluid, a symmetric and steady field was observed. Whereas, for viscoelastic fluids, it was observed that a transition from steady and symmetric flow to an unsteady and asymmetric flow took place when the Weissenberg number crossed a critical limit.

Mustapha et al. (2023)	Thermosolute free convection in porous, isotropic media filled with Casson nano fluid (Aluminium nano particles) subjected to a magnetic field was studied. Extended Darcy law of Brinkman-Forchhiemer was employed to model the flow, and the equations were solved by finite volume method. It was observed that mass and heat transport increased with an increase in the Casson fluid parameter. This increase is significant when the Casson fluid parameter lies in the range of 0.1- 0.4.
Khan and Sasmal (2023)	Electro kinetic transport of visco-elastic and Newtonian fluids in model porous media with long micro pores was studied. Numerical solutions for both Newtonian and viscoelastic fluids were obtained. Over the entire range of parameters considered in the study, a steady and symmetrical velocity field was observed for Newtonian fluids. For viscoelastic fluids, a transition from symmetric and steady to an unsteady and asymmetric profile takes place when the Weissenbarg number crosses a critical limit.
Das and Ojha (2018)	In this study, MHD flow of a viscoelastic fluid between two porous parallel plates under the action of a pressure gradient which was sinusoidal, was examined. The governing partial differential equations were solved analytically. Results indicated that oscillating pressure gradient with low frequency prevents the back flow and skin friction was reduced significantly by embedding the channel in porous medium.
Radnia and Nazar (2017)	Heat transfer of Power law fluid flowing over a moving surface was examined considering uniform injection/suction. The surface was subjected to uniform temperature. Merk-Chao series was employed and a set of ordinary differential equations were obtained. Results revealed that thickness of thermal boundary layers of pseudo plastic fluids are higher than the dialatant fluids. Internal heat generation increased the thermal boundary layer thickness.
Madhy (2016)	Magnetohydrodynamic flow in a Casson fluid with slip condition, with a stretching sheet, under the effect of injection/suction was studied. The partial differential equations describing the flow and heat transfer effect were reduced to a set of ordinary differential equations by a similarity transformation method and were solved numerically. It was reported that an increment in the Casson parameter suppresses the velocity field. Temperature, on the other hand, is increased with an increase in the Casson parameter.
Adesanya and Falade (2015)	Entropy generation rate in MHD flow of a third-grade fluid in parallel plates, with porous media, was studied. The flow was actuated by applied constant pressure gradient and influenced by the applied magnetic field. The equations were solved using the perturbation method.
Hayat et al. (2008)	Magnetohydrodynamic flow of third grade fluid through a porous channel was studied. Analytical solution for velocity was yielded by applying homotopy analysis method. Effect of different parameters on velocity were analyzed.

From the review of the previous studies presented in Table 1, it is clear that studies on the flow of various non-Newtonian fluids through different geometries like parallel plates, channels, and pipes with suction/injection through porous walls are still an active area of research. Numerous studies have been conducted on Casson fluids, Power law fluids, and Visco-elastic fluids in this direction. However, studies on third-grade fluid flow through channels and parallel plates with suction/injection through porous walls are scarce in open literature. Further, studies employing LSM for solving non-linear governing equations arising in this field are also rare. In view of these, in the current study, the flow of a third-grade fluid through large parallel plates with uniform suction/injection through the porous walls is considered. The novelties of the current study are the following:

- Study of the effect of uniform suction/injection on the velocity field for a third-grade fluid flow through large parallel plates.
- Study of the impact of the third-grade fluid parameter on the velocity field in the presence of the wall injection/suction.
- Implementation of the LSM in this case, where the velocity field distorts from symmetrical nature to asymmetry due to the cross-flow. This requires very tricky selection of the trial function for LSM and this selection process may be useful for

applying LSM in similar situations where velocity field is not symmetric about the central axis of the plate/channel.

- Presenting a semi-analytical solution of the equation, for which no exact analytical or approximate analytical solution is reported. For second-grade fluid in similar flow condition, the exact solution is admissible, which was reported. But in the case of third-grade fluid, no exact solution is reported for which a semi-analytical solution with high accuracy is obtained by LSM.
- Flow rate per unit width of the plates are obtained, which is an important parameter from engineering point of view. Impact of third grade fluid parameter, cross-flow Reynolds number on the flow rate is discussed.

2. Problem Formulation

The problem under consideration is represented in Fig. 1. The frame of reference is chosen as shown in Fig. 1. The upper and lower plates are porous, and fluid is injected at the lower plate and sucked at the upper plate with uniform velocity. The flow is taking place along *x* direction, and due to the imposed pressure gradient flow takes place along *x*. The parallel plates are assumed to be very large along the *z*-direction. The flow is considered to be laminar, incompressible, steady and hydro-dynamically fully developed.

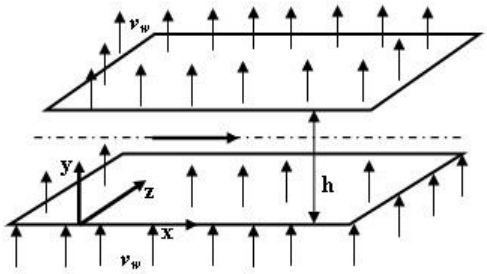

Fig. 1. Pictorial representation of the flow through parallel porous plates

The continuity equation [25, 27] is given below as:

$$\nabla.V = 0 \tag{1}$$

where V is the velocity vector. Neglecting body forces, the momentum conservation equation [25, 27] in vector form is given below as follows:

$$\rho\frac{DV}{Dt} = \nabla.\tau \tag{2}$$

where τ is the stress tensor. The relation between the stress tensor and rate of deformation tensor [25-28] for a third-grade fluid is given by the following:

$$\begin{aligned}\tau = &-pI + \mu A_1 + \alpha_1 A_2 + \alpha_2 A_1^2 + \beta_1 A_3 \\ &+ \beta_2\left(A_1A_2 + A_2A_1\right) + \beta_3\left(trA_1^2\right)A_1\end{aligned} \tag{3}$$

where, p is the static pressure, μ, β_1, β_2, and β_3 are the material constants of third-grade fluids. A_1, A_2, A_3 are given by the following relations [25, 27]:

$$A_1 = \left(gradV\right) + \left(gradV\right)^T \tag{4}$$

In general, A_n is given by the following relation [25, 27]:

$$A_n = \frac{DA_{n-1}}{Dt} + A_{n-1}\left(gradV\right) + \left(gradV\right)^T A_{n-1}, n = 2,3 \tag{5}$$

As the plates are very wide along the lateral direction, the velocity component u is independent of z. Further, a fully developed flow assumption leads us to search for a solution of the following form:

$$V = \left[u(y), 0, 0\right] \tag{6}$$

Now, From Eq. (2), using Eq. (3)-Eq. (6), we have the momentum conservation equations in the x, y and z directions as follows:

$$\mu\frac{d^2u}{dy^2} + 6\left(\beta_2+\beta_3\right)\frac{d^2u}{dy^2}\left(\frac{du}{dy}\right)^2 - \frac{\partial p}{\partial x} = \rho v\frac{du}{dy} \tag{7}$$

$$\left(2\alpha_1+\alpha_2\right)\frac{d}{dy}\left[\left(\frac{du}{dy}\right)^2\right] = \frac{\partial p}{\partial y} \tag{8}$$

$$\frac{\partial p}{\partial z} = 0 \tag{9}$$

Boundary conditions [24]:

$$u(0) = u(h) = 0 \tag{10.1}$$

$$v(0) = v(h) = v_w \tag{10.2}$$

From the boundary condition given by Eq. (10.2) for uniform blowing and suction, the y component of velocity v in the flow regime between the plates can be approximated as follows [24]:

$$v \approx v_w \tag{11}$$

Therefore, Eq. (7) reduces to the following:

$$\mu\frac{d^2u}{dy^2} + 6\left(\beta_2+\beta_3\right)\frac{d^2u}{dy^2}\left(\frac{du}{dy}\right)^3 - \rho v_w\frac{du}{dy} = \frac{\partial p}{\partial x} \tag{12}$$

From Eq. (9), we get the p is independent of z. Then, from Eq. (8), the following relation for p is obtained:

$$p = \int_0^y (2\alpha_1 + \alpha_2)\frac{d}{dy}\left[\left(\frac{du}{dy}\right)^2\right]dy + f(x) + c \quad (13)$$

where c is an integral constant. From Eq. (13), it is evident that $\frac{\partial p}{\partial x}$ is dependent on x alone and can be replaced as $\frac{dp}{dx}$. Therefore, Eq. (12) reduces to the following form:

$$\mu\frac{d^2u}{dy^2} + 6(\beta_2 + \beta_3)\frac{d^2u}{dy^2}\left(\frac{du}{dy}\right)^3 - \rho v_w\frac{du}{dy} = \frac{dp}{dx} \quad (14)$$

The left-hand side of Eq. (14) is dependent on y alone, as u depends only on y as per the assumption. The right-hand side of Eq. (14) depends on x only. The only possibility is that both sides are equal to a constant. For reducing Eq. (14) and boundary conditions in their dimensionless forms, dimensionless variables and parameters introduced are as follows:

Dimensionless variables and parameters;

$$\left.\begin{aligned} &y^* = \frac{y}{h}, u^* = \frac{u}{U_0}, \\ &A = \left[\frac{(\beta_2 + \beta_3)U_0^2}{\mu h^2}\right], \\ &\mathrm{Re} = \frac{\rho v_w h}{\mu}, N = \frac{dp}{dx}\frac{h^2}{\mu U_0} \end{aligned}\right\} \quad (15)$$

where y^* and u^* are the dimensionless y coordinate and velocity along the flow direction. A is the third-grade fluid parameter, where A=0 corresponds the case for Newtonian fluids. Re is the cross-flow Reynolds number based on the uniform wall blowing and suction velocity, and N is a measure of non-dimensional pressure gradient. In the current study, the reference velocity U_0 [24] can be considered as follows:

$$U_0 = -\left(\frac{dp}{dx}\right)\frac{h^2}{\mu} \quad (16)$$

Therefore, N reduces as follows:

$$N = -1 \quad (17)$$

Using the dimensionless variables and parameters, the non-dimensional equation is obtained as follows:

$$\frac{d^2u^*}{dy^{*2}} + 6A\frac{d^2u^*}{dy^{*2}}\left(\frac{du^*}{dy^*}\right)^2 - (-1) = \mathrm{Re}\frac{du^*}{dy^*} \quad (18)$$

Dimensionless boundary conditions:

$$u^*(0) = u^*(1) = 0 \quad (19)$$

For the sake of convenience, omitting the asterisk, we get the non-dimensional governing equation and boundary conditions as follows:

$$\frac{d^2u}{dy^2} + 6A\frac{d^2u}{dy^2}\left(\frac{du}{dy}\right)^2 + 1 = \mathrm{Re}\frac{du}{dy} \quad (20)$$

$$u(0) = u(1) = 0 \quad (21)$$

3. Solution

3.1. Solution by LSM:

Equation (20) is a non-linear, ordinary differential equation for which getting an exact analytical solution may not be possible. LSM is a highly effective semi-analytical technique that produces a very accurate approximate solution. For applying LSM, first, trial functions or base functions have to be chosen. In the present study, the trial functions have to be chosen very carefully. From the solution of the Newtonian fluid flow problem, it is known that when the cross-flow Reynolds number is 0, then the velocity profile is symmetric about the centerline of the parallel plates. With the increase in Re, the velocity profile deviates from symmetry and displays an asymmetric pattern. In view of this, the approximate solution is to be chosen as a combination of symmetric and asymmetric functions with respect to the centerline of the parallel plate channel. Therefore, the base/trial functions $y^2(1-y), y^3(1-y)$ are chosen, which are asymmetric functions and $y(1-y)$ is the symmetric function (symmetric with respect to the centre line of the channel). The trial functions are picked up such that the boundary conditions given by Eq. (21) are satisfied. Therefore, the approximate solution is chosen as a combination of all these asymmetric and symmetric functions. c_1, c_2 and c_3 are the constants to be evaluated. When the velocity profile deviates from symmetry, c_3 should decrease and c_1 and c_2 should increase. When the cross-flow Reynolds number decreases, the reverse should occur. In view of these, the following approximate solution is chosen for Eq. (20) [3].

$$u = c_1y^2(1-y) + c_2y^3(1-y) + c_3y(1-y) \quad (22)$$

Upon substitution of Eq. (22) in Eq. (20), the residual function results as follows:

$$\frac{d^2u}{dy^2} + 6A\frac{d^2u}{dy^2}\left(\frac{du}{dy}\right)^2 + 1 - \mathrm{Re}\frac{du}{dy} = R \quad (23)$$

In the present study, all steps of LSM are carried out by the Symbolic Computation tool of MATLAB. The residual R as obtained in MATLAB is presented below as:

$$\begin{aligned} R(y,c_1,c_2,c_3) &= (-1) - 2c_3 - 4c_1 y - 2c_1(y-1) \\ &-6c_2 y^2 + \mathrm{Re}\begin{bmatrix} c_3 y + c_3(y-1) + c_1 y^2 + c_2 y^3 \\ +2c_1 y(y-1) \\ +3c_2\, y^2(y-1) \end{bmatrix} \\ &-6c_2 y(y-1) - 6A\begin{bmatrix} 2c_3 + 4c_1 y + 2c_1(y-1) \\ +6c_2 y^2 + 6c_2 y(y-1) \end{bmatrix} \\ &\begin{bmatrix} c_3 y + c_3(y-1) + c_1 y^2 + \\ c_2 y^3 + 2c_1 y(y-1) + 3c_2 y^2(y-1) \end{bmatrix}^2 \end{aligned} \tag{24}$$

Now, as per the requirement of LSM [3, 29], the summation of the square of the error or residual (R) is to be obtained over the entire domain. This is accomplished as follows:

$$S = \int_0^1 R^2 dy \tag{25}$$

Then, the next task is to minimize S with respect to the unknowns c_1, c_2 and c_3. This will generate three non-linear, coupled algebraic equations. The equations [3, 29] are generated as follows:

$$\frac{\partial S}{\partial c_1} = \frac{\partial}{\partial c_1}\left(\int_0^1 R^2 dy\right) = \int_0^1 R\frac{\partial R}{\partial c_1} dy = 0 \tag{26}$$

$$\frac{\partial S}{\partial c_2} = \frac{\partial}{\partial c_2}\left(\int_0^1 R^2 dy\right) = \int_0^1 R\frac{\partial R}{\partial c_2} dy = 0 \tag{27}$$

$$\frac{\partial S}{\partial c_3} = \frac{\partial}{\partial c_3}\left(\int_0^1 R^2 dy\right) = \int_0^1 R\frac{\partial R}{\partial c_3} dy = 0 \tag{28}$$

Equation (26)-Eq. (28) lead to the following equations:

$$\begin{aligned} &\frac{33336A^2c_1^5}{385} + \frac{210768}{455}A^2c_1^4c_2 + \frac{30672}{77}c_1^4c_3 + \frac{449928}{455}c_1^3c_2^2 + \frac{659184}{385}c_1^3c_2c_3 + \frac{25488}{35}A^2c_1^3c_3^2 \\ &+ \frac{478944}{455}A^2c_1^2c_2^3 + \frac{1252584}{455}A^2c_1^2c_2^2c_3 + \frac{908064}{385}A^2c_1^2c_2c_3^2 + \frac{23112}{35}A^2c_1^2c_3^3 \\ &+ \frac{559296}{1001}A^2c_1c_2^4 + \frac{892512}{455}A^2c_1c_2^3c_3 + \frac{978048}{385}A^2c_1c_2^2c_3^2 + \frac{10032}{7}A^2c_1c_2c_3^3 \\ &+ \frac{10368}{35}A^2c_1c_3^4 + \frac{10067328}{85085}A^2c_2^5 + \frac{523080}{1001}A^2c_2^4c_3 + \frac{4550976}{5005}A^2c_2^3c_3^2 \\ &+ \frac{298728}{385}A^2c_2^2c_3^3 + \frac{11328}{35}A^2c_2c_3^4 + \frac{360}{7}A^2c_3^5 + 6A\,\mathrm{Re}c_1^3 + 18A\,\mathrm{Re}c_1^2c_2 \\ &-18A\,\mathrm{Re}c_1^2c_3 - 18A\,\mathrm{Re}c_1c_2^2 - 36A\,\mathrm{Re}c_1c_2c_3 - 18A\,\mathrm{Re}c_1c_3^2 - 6A\,\mathrm{Re}c_2^3 - 18A\,\mathrm{Re}c_2^2c_3 \\ &-18A\,\mathrm{Re}c_2c_3^2 - 6A\,\mathrm{Re}c_3^3 + \frac{1116}{35}Ac_1^3 + \frac{3672}{35}Ac_1^2c_2 + \frac{2928}{35}Ac_1^2c_3 - 6(-1)Ac_1^2 \\ &+ \frac{804}{7}Ac_1c_2^2 + \frac{1296}{7}Ac_1c_2c_3 - 12(-1)Ac_1c_2 + 72Ac_1c_3^2 + 12(-1)Ac_1c_3 + \frac{3216}{77}Ac_2^3 \\ &+ \frac{3576}{35}Ac_2^2c_3 - 6(-1)Ac_2^2 + \frac{2832}{35}Ac_2c_3^2 + 12(-1)Ac_2c_3 + \frac{96}{5}Ac_3^3 - 6(-1)Ac_3^2 \\ &+ \frac{\mathrm{Re}^2}{10}c_1 + \frac{3}{35}\mathrm{Re}^2c_2 + \frac{1}{10}\mathrm{Re}^2c_3 - \mathrm{Re}(c_1+c_2+c_3) + 4c_1 + \frac{24}{5}c_2 + 2c_3 - (-1) = 0 \end{aligned} \tag{29}$$

$$\frac{\left(31104A^2c_1^5\right)}{385}+\frac{\left(33336A^2c_1^4c_2\right)}{77}+\frac{\left(2592A^2c_1^4c_3\right)}{7}+\frac{\left(421536A^2c_1^3c_2^2\right)}{455}+\frac{\left(122688A^2c_1^3c_2^2c_3\right)}{77}+\frac{\left(23616A^2c_1^3c_3^2\right)}{35}$$
$$+\frac{\left(449928A^2c_1^2c_2^3\right)}{455}+\frac{\left(988776A^2c_1^2c_2^2c_3\right)}{385}+\frac{\left(96464A^2c_1^2c_2c_3^2\right)}{35}+\frac{\left(21384A^2c_1^2c_3^3\right)}{35}+\frac{\left(239472A^2c_1c_2^4\right)}{455}$$
$$+\frac{\left(908064A^2c_1c_2^2c_3^2\right)}{385}+\frac{\left(835056A^2c_1c_2^3c_3\right)}{455}+\frac{\left(46224A^2c_1c_3^3c_2\right)}{35}+\frac{\left(9648A^2c_1c_3^4\right)}{35}+\frac{\left(559296A^2c_2^5\right)}{5005}$$
$$+\frac{\left(223128A^2c_2^4c_3\right)}{455}\frac{\left(223128A^2c_2^4c_3\right)}{455}+\frac{\left(326016A^2c_2^3c_3^2\right)}{385}+\frac{\left(5016A^2c_2^2c_3^3\right)}{7}+\frac{\left(10368A^2c_2c_3^4\right)}{35}+\frac{\left(216A^2c_3^5\right)}{5}$$
$$-\left(6A^2\,\mathrm{R_e}\,c_1^3\right)-\left(18A\,\mathrm{R_e}\,c_1^2c_2\right)-\left(18A\,\mathrm{R_e}\,c_1^2c_3\right)-\left(18A\,\mathrm{R_e}\,c_2^2c_1\right)-\left(36A\,\mathrm{R_e}\,c_1c_2c_3\right)-\left(18A\,\mathrm{R_e}\,c_1c_3^2\right) \quad (30)$$
$$-\left(6A\,\mathrm{R_e}\,c_2^3\right)-\left(18A\,\mathrm{R_e}\,c_2^2c_3\right)-\left(18A\,\mathrm{R_e}\,c_3^2c_2\right)-\left(6A\,\mathrm{R_e}\,c_3^3\right)+\frac{\left(1024Ac_1^3\right)}{35}+\frac{\left(3348Ac_1^2c_2\right)}{35}+\frac{\left(384Ac_1^2c_3\right)}{5}$$
$$-\left(6NAc_1^2\right)+\frac{\left(3672Ac_2^2c_1\right)}{35}+\frac{\left(5856Ac_2c_1c_3\right)}{35}-\left(-12Ac_1c_2\right)+\frac{\left(336Ac_3^2c_1\right)}{5}-\left(-12Ac_1c_3\right)+\frac{\left(268Ac_3^2\right)}{7}$$
$$+\frac{\left(648Ac_2^2c_3\right)}{7}-\left(-6Ac_2^2\right)+\left(72Ac_3^2c_2\right)-12(-1)Ac_2c_3+16Ac_3^3-6(-1)Ac_3^2$$
$$+\frac{2\,\mathrm{Re}^2c_1}{15}+\frac{\mathrm{Re}^2c_2}{10}+\frac{\mathrm{Re}^2c_3}{6}-\mathrm{Re}c_1-\mathrm{Re}c_2-\mathrm{Re}c_3+4c_2+2c_3-(-1)=0$$

$$\frac{2592}{35}A^2c_1^5+\frac{30672}{77}A^2c_1^4c_2+\frac{11808}{35}A^2c_1^4c_3+\frac{329592}{385}A^2c_1^3c_2^2+\frac{50976}{35}A^2c_1^3c_2+\frac{21384}{35}A^2c_1^3c_3^2$$
$$+\frac{417528}{455}A^2c_1^2c_2^3+\frac{908064}{385}A^2c_1^2c_2^2c_3+\frac{69336}{35}A^2c_1^2c_2c_3^2+\frac{19296}{35}A^2c_1^2c_3^3$$
$$\frac{22318}{455}A^2c_1c_2^4+\frac{652032}{385}A^2c_1c_2^3c_3+\frac{15048}{7}A^2c_1c_2^2c_3^2+\frac{41472}{35}A^2c_1c_2c_3^3$$
$$+216A^2c_1c_3^4+\frac{104616}{1001}A^2c_2^5+\frac{2275488}{5005}A^2c_2^4c_3+\frac{298728}{385}A^2c_2^3c_3^2$$
$$+\frac{22656}{35}A^2c_2^2c_3^3+\frac{1800}{7}A^2c_2c_3^4+\frac{432}{5}A^2c_3^5+6A\,\mathrm{Re}c_1^3-18A\,\mathrm{Re}c_1^2c_2 \quad (31)$$
$$-6A\,\mathrm{Re}c_2^3-18A\,\mathrm{Re}c_2^2c_3+18A\,\mathrm{Re}c_2c_3^2+\frac{128}{7}Ac_1^3+\frac{2928}{35}Ac_1^2c_2+\frac{336}{5}Ac_1^2c_3$$
$$-6(-1)Ac_1^2+\frac{648}{7}Ac_1c_2^2+144Ac_1c_2c_3-12(-1)Ac_1c_2+48Ac_1c_3^2-12(-1)Ac_1c_3$$
$$+\frac{1192}{35}Ac_3^3+\frac{2832}{35}Ac_2^2c_3+6A(-1)c_2^2+\frac{288}{5}Ac_3^2c_2-12(-1)Ac_2c_3+32Ac_3^3$$
$$-12(-1)Ac_3^2+\frac{1}{6}\mathrm{Re}^2c_1+\frac{1}{10}\mathrm{Re}^2c_2+\frac{1}{3}\mathrm{Re}^2c_3-\mathrm{Re}(c_1+c_2)+2(c_1+c_2)+4c_3-2(-1)=0$$

Equation (29)-Eq. (31) is a set of coupled non-linear algebraic equations. This set is solved by the Symbolic computation tool of MATLAB. The solution depends on A, Re.

As stated earlier, when Re=0, A=0, c_1=0, c_2= 0 and c_3=0.5. When Re=1, A= 0, c_1=0.1232, c_2= 0.0407 and c_3= 0.418. When, the cross-flow Reynolds number is zero indicating no suction/injection, then the contribution of c_1 and c_2 is zero, and that of c_3 is 100%. When the cross-flow Reynolds number increases, the contribution of c_3 decreases and the contribution of the other constants increase.

3.2. Solution by Perturbation Method:

Another solution to the governing equation is yielded by the traditional perturbation method. The traditional perturbation method is a very popular analytical technique that is still in use today. This is used to find the analytical solution of non-linear partial differential equations and ordinary differential equations. In the present study, the perturbation method is used to obtain the solution of the governing equation for small values of the cross-flow Re and the non-Newtonian parameter A. For implementing the

perturbation method, Re and *A* are considered to be small and used as a perturbation parameter.

$$\frac{d^2u}{dy^2}-\varepsilon\frac{du}{dy}+6\varepsilon\frac{d^2u}{dy^2}\left(\frac{du}{dy}\right)^2-(-1)=0 \tag{32}$$

In Eq. (32), Re=*A*= ε is substituted. For implementing the perturbation method, the solution for *u* is assumed to be as follows:

$$u=u_0+\varepsilon u_1+\varepsilon^2u_2+\ldots \tag{33}$$

Where a solution for the second order is considered. Following the standard procedure of the perturbation method, putting Eq. (33) in Eq. (32) and combining the coefficients of ε^0, $\varepsilon^1$and ε^2 and equating zero, 0th order, 1st order and 2nd order equations are as follows:
0th order equation:

$$\frac{d^2u_0}{dy^2}=-1 \tag{34}$$

For obtaining the boundary conditions, Eq. (33) is substituted in Eq. (21), and the coefficients of ε^0, $\varepsilon^1$and ε^2 are equated to zero, and the boundary conditions required are given below:

Boundary conditions:

$$u_0(0)=0,u_0(1)=0 \tag{35}$$

1st order equation:

$$\frac{d^2u_1}{dy^2}-\frac{du_0}{dy}+6\frac{d^2u_0}{dy^2}\left(\frac{du_0}{dy}\right)^2=0 \tag{36}$$

Boundary conditions:

$$u_1(0)=0,u_1(1)=0 \tag{37}$$

2nd order equation:

$$\frac{d^2u_2}{dy^2}-\frac{du_1}{dy}+6\frac{d^2u_1}{dy^2}\left(\frac{du_0}{dy}\right)^2+12\frac{d^2u_0}{dy^2}\frac{du_0}{dy}\frac{du_1}{dy}=0 \tag{38}$$

Boundary conditions:

$$u_2(0)=0,u_2(1)=0 \tag{39}$$

Solutions:

Equation (34), Eq. (36) and Eq. (39) along with the boundary conditions are solved to obtain the 0th order, 1st order and 2nd order solutions as follows:

0th order solution:

$$u_0=\frac{(-1)}{2}(y^2-1) \tag{40}$$

1st order solution:

$$u_1=\frac{(-1)}{2}\left[\frac{1}{3}\left(y^3-y\right)-\frac{1}{2}\left(y^2-y\right)\right]-\frac{1}{2}(-1)^3\left(y^4-y\right)-\frac{3}{2}(-1)^3\left(-\frac{2}{3}\right)\left(y^3-y\right)-\frac{3}{2}(-1)^3\left(\frac{1}{2}\right)\left(y^2-y\right) \tag{41}$$

$$u_2=\frac{(-1)}{2}\left(\frac{y^4}{12}-\frac{y^3}{6}\right)-\frac{3}{2}(-1)^3\left(\frac{y^5}{15}-\frac{y^4}{2}+\frac{y^3}{6}\right)+\left[\frac{-1}{12}+\frac{(-1)^3}{4}\right]\frac{y^2}{2}-6(-1)^2\left[\begin{array}{l}\frac{-1}{2}\left(\frac{y^5}{10}-\frac{y^4}{4}+\frac{y^3}{6}\right)-\frac{3}{2}(-1)^3\\ \left(\frac{8}{90}y^6-\frac{16}{60}y^5+\frac{y^4}{4}-\frac{y^3}{6}\right)\\ +\left(\frac{y^3}{3}-\frac{y^2}{2}\right)\left(\frac{-1}{12}-\frac{1}{4}\right)\end{array}\right]-\frac{-3}{2}(-1)^2\left[\begin{array}{l}\left(\frac{8}{20}y^5-y^4+y^3-\frac{y^2}{2}\right)\left(\frac{-1}{2}\right)\\ +\frac{3}{2}\left(\frac{16}{30}y^6+2y^4+\frac{y^2}{2}-\frac{8}{5}y^5\right)\end{array}\right]+\frac{131}{72}y \tag{42}$$

The final solution for *u* is obtained by substituting u_0, u_1 and u_2 from the Eq. (40), Eq. (41) and Eq. (42) in Eq. (33).

3.3. Solution for Newtonian fluids:

If *A*=0 is substituted in Eq. (20), the governing equation for Newtonian fluids is retrieved, which is given below:

$$\frac{d^2u}{dy^2}-\mathrm{Re}\frac{du}{dy}=-1 \tag{43}$$

The boundary condition remains the same as given by Eq. (21). The solution to Eq. (43) with the boundary conditions given by Eq. (21) is given as follows:

$$u=\frac{1}{\mathrm{Re}\left(e^{\mathrm{Re}}-1\right)}\left[1-e^{\mathrm{Re}y}\right]+\frac{y}{\mathrm{Re}} \tag{44}$$

3.4. Dimensionless Flow Rate:

In this study, the flow rate per unit width of the plate is obtained, and the influence of the third-grade fluid parameter and the cross-flow Reynolds number on the flow rate is studied. The limitation of this result is that it is only valid near the central region of the plates. Due to the large plate assumption, the variation of the axial velocity in the lateral direction is not considered. The dimensionless flow rate per unit width is calculated as follows:

$$q=\int_0^1 u\,dy \tag{45}$$

where, $q = \frac{q^*}{U_0 h}$, q^* is the dimensional flow rate.

By substituting the expression for u from Eq. (22) to Eq. (44), the dimensionless flow rate is obtained as follows:

$$q = \frac{c_1}{12} + \frac{c_2}{20} + \frac{c_3}{6} \tag{46}$$

For different values of A and Re, dimensionless flow rate can be evaluated from Eq. (46).

Dimensionless shear stresses [25, 27] at the upper plate and lower plates are as follows:

$$\tau_{uw} = \left(\frac{du}{dy}\right)_{y=1} + 2A\left(\frac{du}{dy}\right)^3_{y=1} \tag{47.1}$$

$$\tau_{lw} = \left(\frac{du}{dy}\right)_{y=0} + 2A\left(\frac{du}{dy}\right)^3_{y=0} \tag{47.2}$$

Substituting the expression for u from Eq. (22) into Eq. (47) yields the following:

$$\tau_{uw} = -(c_1 + c_2 + c_3) + 2A\left[-(c_1 + c_2 + c_3)\right]^3 \tag{48.1}$$

$$\tau_{lw} = c_3 + 2Ac_3^3 \tag{48.2}$$

4. Results and Discussion

In this section, the effects of different parameters like a third-grade fluid parameter and cross-flow Reynolds number on the velocity distribution are analyzed. Before that, validation of the results has to be carried out. In the present study, a solution of the velocity distribution is obtained by LSM and the traditional perturbation method. The outcome of the perturbation method is valid for small parameters only. Therefore, a comparison of the outcomes of LSM and perturbation methods is made for small parameters. Further, outcomes of the LSM are compared with those Newtonian fluids in the limiting case of the non-Newtonian parameter as zero. The comparisons are shown in Fig.2 (a) and Fig. 2(b).

Fig. 2(a) presents the comparison of the results of the LSM (with the non-Newtonian parameter as zero) and the results of Newtonian fluids for which an exact solution is available. It is evident that the results exactly match. Figure 2(b) presents the comparison of the results of LSM and the perturbation solution obtained in the present study. It is clear that the results are closely matching. This comparison establishes the validity of the results of the current study. In the current study, the cross-flow Reynolds (Re) number has been chosen in the range of 0-4. The third-grade fluid parameter A varies nearly in the range of 0-0.3.

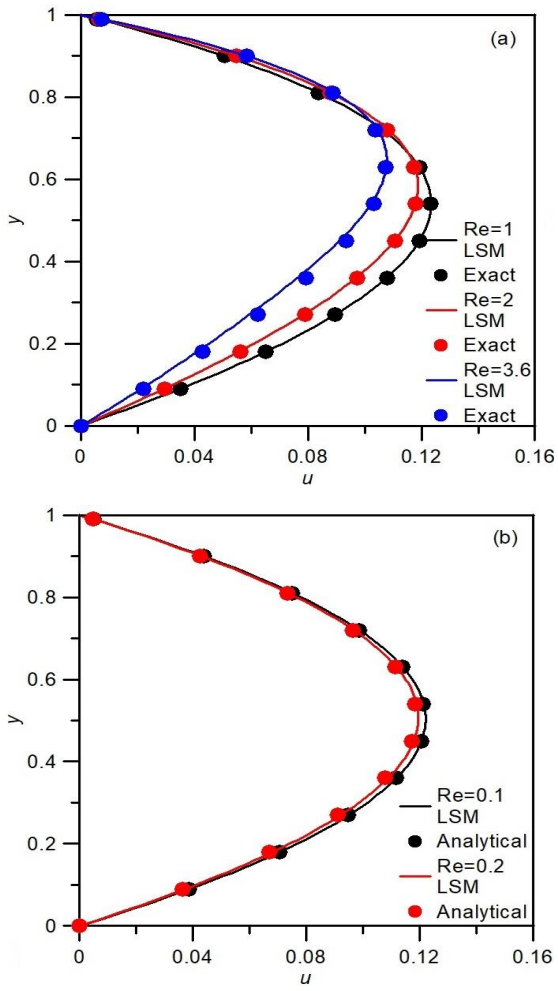

Fig. 2. (a) Comparison of the velocity distributions, (b) Comparison of the from the Exact analytical solution velocity distributions from the and LSM for Newtonian fluids LSM and perturbation method.

In Fig.3 (a), dimensionless velocity distributions for different non-Newtonian parameters are plotted when the cross-flow Reynolds number is fixed at 0.1. It is observed that velocity profiles are nearly symmetric about the central axis of the plates for all values of A. This is the result of a very low Reynolds number (Re=0.1), which indicates very low injection/suction velocity through the porous walls. It is evident with increase in A, velocity decreases. From Eq. (15), it is clear that A can increase in various ways. A can increase if β_2 or β_3 increase, keeping other parameters unchanged. Increase in β_2 or β_3 signifies increase in the flow resistance, which will result in a decrease in velocity. Therefore, velocity will decrease with an increase in A. Again, from Eq.

(15), we conclude that if μ decreases, then also *A* can increase. If μ decreases, to keep Re fixed, *h* has to be reduced in the same order. This will result in a reduction in the reference velocity. This will also result in a decrease in the gap between the parallel plates, causing a higher flow resistance for fixed values of β_2 or β_3. Therefore, if *A* increases as result of a decrease in μ, velocity should decrease which is displayed in Fig. 3 (a).

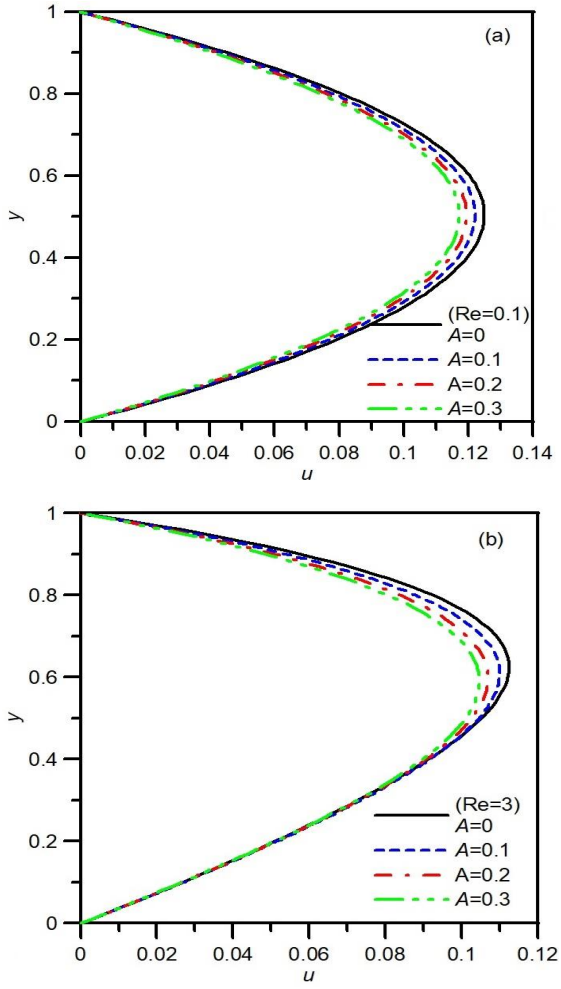

Fig. 3. (a) Velocity distribution (non-dimensional), (b) Velocity distribution for different A when Re is fixed at 0.1 (non-dimensional) for different A when Re is fixed at 3

In Fig.3 (b), dimensionless velocity distributions for different *A* are plotted for a higher cross-flow Reynolds number (Re=3). As displayed for Newtonian fluids, in the present case of third-grade fluid also, velocity profiles are distorted from their symmetric nature about the central axis of the plates for higher values of the cross-flow Reynolds number.

The point of occurrence of the peak velocity is shifted towards the upper plate when the injection is through the lower plate. With increase in *A*, velocity decreases as explained earlier. But it is important to note that velocity is nearly unaffected by any change in *A*, starting from *y*=0.4 up to the lower plate. Of course, depending on Re, the value of *y* from where the velocity is unaffected by any change in *A* will differ in magnitude. For higher values of Re, the injection velocity is higher at the lower plate. Consequently, the flow resistance is higher and axial velocity near the wall is lower. With the increase in *A*, resistance increases further and up to a higher region from the plate; velocity remains low and is unaffected by changes in *A*. Another important observation is the shifting of the maximum velocity towards the central region with an increase in *A*. With the rise in *A*, velocity decreases which results in this shift of the maximum velocity. A similar trend was observed in the study of Ariel [24]. When Re=0.1, the maximum velocity decreases from 0.12 to 0.11 with a change in *A* from 0 to 3. Whereas, when Re=3, velocity changes from 0.11 to 0.09 when *A* changes from 0 to 3.

Fig. 4 (a) and Fig. 4 (b) depict non-dimensional velocity distributions for different values of Re with unchanged values of *A*. Like Newtonian fluids, with an increase in Re, velocity near the lower plate decreases due to higher values of injection, whereas near the upper plate, velocity increases due to higher values of suction in the wall. However, this increase in velocity near the upper plate is resisted with an increase in *A*, as shown in Fig. 4 (b). For *A*=0.3 and Re=3, velocity near the lower plate (from y=0.7) is higher than the velocity for Re=0. But the increment is less compared to the increment in the case of *A*=0.04 when Re changes from 0 to 3, as depicted in Fig. 4 (a). For higher *A*, due to an increase in flow resistance, velocity is lower. Therefore, when Re changes to 3, velocity increases near the lower plate, but the rate of increase is comparatively less (compared to the case of *A*=0.04). With further rise in *A*, this rate of increment of velocity with an increase in Re is still lower near the upper plate. Higher values of *A*, suppress the boundary layer thickness near the upper plate with increase in cross-flow Reynolds number. But higher values of *A*, increase the boundary layer thickness near the lower plate for higher values of the cross-flow Reynolds number.

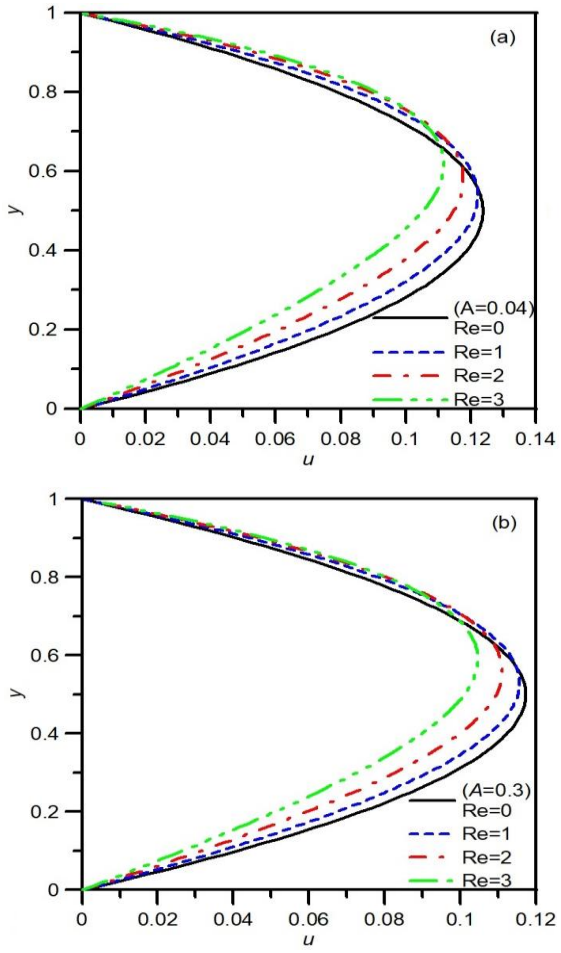

Fig. 4. (a)Velocity distribution (non-dimensional), (b) Velocity Distribution (dimensionless) for different Re with A =0.04 for different Re with A=0.3

It is important to discuss the effect of flow passage in the porous wall on velocity. If the area of the flow passage in the porous walls increases, then more mass transfer occurs towards the axially flowing fluid through the parallel plate. This increases the cross-flow Reynolds number. Increase in cross-flow Reynolds number will increase the boundary layer thickness near the lower wall and the reverse will take place near the upper wall. Consequently, shear stress in the lower wall will decrease and in the upper wall, shear stress will increase. With the increase in cross-flow mass transfer, axial velocity reduces.

Variation of dimensionless flow rate per unit width with *A* for different Re is depicted in Fig. 5. From Fig.4 (a) and Fig. 4 (b), it is observed that with increment in *A*, velocity decreases for all values of Re. Therefore, the flow rate will be reduced for higher *A*. When Re increases, for all *A*, for most of the portion of the channel gap, velocity is reduced only with an increase near the upper plate (for top suction and bottom injection). Therefore, the flow rate decreases with an increase in Re. It is noted from Fig. 5 that the rate of decrease is higher for higher values of Re. That is, the decrement in flow rate is higher when Re changes from 2 to 3, compared to the case when Re changes from 0 to 1 or 1 to 2.

The variation of wall shear stresses with Re for different *A* is plotted in Fig.6. It is clear from Fig. 6 that shear stress at the upper plate is more sensitive towards change in *A* compared to the sensitivity of shear at the lower wall. The shear stress at the lower wall is nearly unaffected by any change in *A*. As already discussed during analyzing the effect of *A* on velocity profiles that, velocity distribution near the lower plate is unaffected by any change in *A*. Consequently, the shear stress is also unaltered by any change in *A*. Of course, shear stress for the third-grade fluid in the upper plate increases with an increase in Re, whereas in the lower plate, it decreases with a rise in Re. This is the same trend as displayed by the Newtonian fluids. Up to A =0.1, the shear stress at the upper plate displays no change. When $A > 0.1$, shear stress at the upper wall changes. In the lower wall, the shear stress is unaltered by any change in *A*.

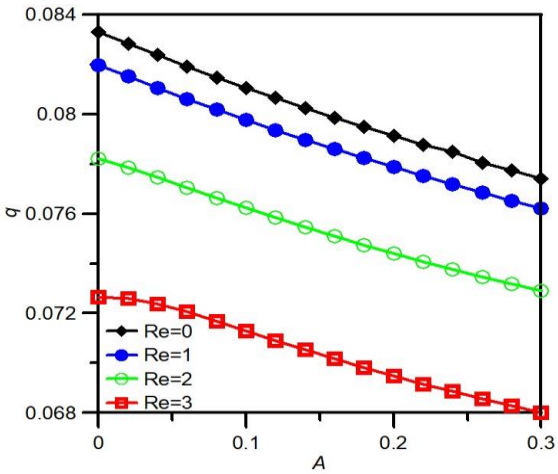

Fig. 5. Variation of dimensionless flow rate per unit width with A for different Re

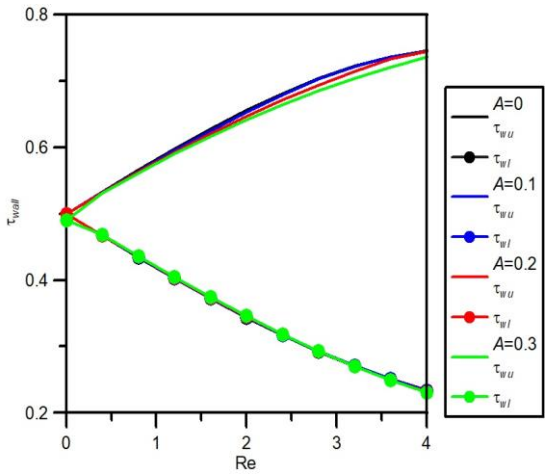

Fig. 6. Variation of dimensionless wall shear stress (upper and lower plates) with Re for different values of A

5. Conclusions

The flow of a third-grade fluid through a parallel plate channel with porous plate and uniform wall blowing/suction is studied. The results will be reversed if top injection and bottom suction are considered. The non-linear momentum conservation equation is solved both by the LSM and perturbation methods. The influence of the third-grade fluid parameter and the cross-flow Reynolds number on the dimensionless velocity distribution, flow rate and the wall shear stress are analyzed. The following important observations are made:

For higher Re, velocity near the lower plate is unaffected by any alteration in A. Near the upper plate, however, velocity decreases with an increase in A. For higher values of A, the maximum velocity shifts towards the central region. When the cross-flow Reynolds number increases, it is known that for injection in the lower wall, boundary layer thickness increases. Near the upper wall with suction, boundary layer thickness decreases. But higher values of the third-grade fluid parameter suppress the boundary layer thickness near the lower wall and increase the boundary layer thickness near the upper wall. With higher values of A, velocity distribution becomes more symmetric about the central axis. When A=0.3, it is observed that for Re=3, velocity is nearly symmetric and displays the characteristics of Newtonian fluids. For higher values of cross-flow Reynolds number, when A decreases from 0.1 to 0, the increase in flow rate is less. This indicates that the rate of increase in flow rate with an increase in A is much less for higher values of the cross-flow of the Reynolds number. Another important outcome is the effect of the passage area of the porous plate on the velocity and shear stress in the lower and upper walls. With the increase in the passage area, due to more cross-flow mass transfer, shear stress in the lower wall decreases, and in the upper wall, shear stress is more.

The shear stress at the upper wall is unaltered for any change in A up to A = 0.1. Shear stress at the upper wall decreases for higher values of A (A >0.2) only. That means for A < 0.1, the shear stress is the same as that of the Newtonian fluids.

The shear stress at the lower wall is unaltered by any change in the non-Newtonian parameter. Shear stress is the same as that of the Newtonian fluids.

The rate of decrease in flow rate is higher for higher values of the cross-flow Reynolds number.

In this study, only the effect of uniform suction/injection on the flow field is studied and how the velocity field is affected is examined. The effect of this flow field on temperature distribution and heat transfer can be examined for further studies. Further, this study can be extended by considering both pressure and shear-driven flow through porous plates (i.e. top plate moving with constant velocity).

Nomenclature

A	Third-grade fluid parameter
A_1, A_2, A_3, A_n	Matrices required for stress and strain rate
C, c_1, c_2, c_3	Constants
h	Gap between the parallel plates (m)
N	Dimensionless pressure gradient
p	Static pressure (Nm^{-2})
q	Dimensionless flow rate (m^3s^{-1})
R	Residual function
Re	Cross-flow Reynolds number
S	Sum of the square of the residuals over the entire domain
t	Time (s)
U_0	Reference velocity (ms^{-1})
u	x component of velocity (ms^{-1})
u_0, u_1, u_2	0^{th} order, 1^{st} order and 2^{nd} order solutions respectively (dimensionless)
u^*	Dimensionless velocity along the axial direction
V	Velocity vector (ms^{-1})
v	y component of velocity (ms^1)
v_w	Velocity of suction/injection (ms^{-1})
x	Coordinate along the flow direction (m)
y	Coordinate perpendicular to the flow (m)direction
y^*	Dimensionless y coordinate
z	Dimensional coordinate along lateral direction

Greek Symbols

α_1, α_2	Material parameter ($Ns^{-3}m^{-3}$)
β_2, β_3	Material parameters (Ns^4m^{-3})
ε	Perturbation parameter
μ	Material parameter(viscosity) (kg m s^{-1})

ρ	Density of the fluid (kg m^{-3})
τ	Stress tensor (Nm^{-2})
τ_{wall}	Dimensionless wall shear stress
τ_{wl}	Lower plate shear stress (dimensionless)
τ_{wu}	Upper plate shear stress (dimensionless)

Funding Statement

This research did not receive any specific grant from funding agencies in the public, commercial, or not-for-profit sectors.

Conflicts of Interest

The author declares that there is no conflict of interest regarding the publication of this article.

References

[1] Ishak, A., Nazar, R., Pop, I., 2008. Uniform suction/blowing effect on flow and heat transfer due to a stretching cylinder. *Applied Mathematical Modeling*, 32 (10), pp. 2059-2066. doi: 10.1016/j.apm.2007.06.036.

[2] Datta, P., Anilkumar, D., Roy, S., Mahani, N. C., 2006. Effect of non-uniform slot injection (suction) on a forced flow over a slender cylinder. *International Journal of Heat and Mass Transfer*, 49 (13), pp. 2366-2371. doi:10.1016/ijheatmasstransfer.2005.10.044.

[3] Mollamahdi M., Abbaszadeh, M., Sheikhzadeh, G.A., 2016. Flow field and heat transfer in a channel with permeable wall filled with Al_2O_3-Cu/Water micro polar hybid nano fluid, effects of chemical reaction and magnetic field. *Journal of Heat and Mass Transfer Research*, 3(2), pp.101-114. doi: 10.22075/JHMTR.2016.447.

[4] Zhou, F., Lee, J., Wang, R., Su, H., 2022. Mechanisms of efficient desalination by a two-dimensional porous nano sheet prepared via bottom-up assembly of cucurbit urils. *Membranes*, 12, p. 12030252. doi: 10.3390/membranes 12030252.

[5] Ali, M., Bostani, M., Rashidi, S., Valipour, M.S., 2023. Challenges and opportunities of desalination with renewable energy resources in middle east countries. *Renewable and Sustainable Energy Review*, 184, pp. 113543. doi: 10.1016/j.rser.2023.113543.

[6] Deghan, M., Rahmani, Y.,Ganji, D.D., Saedodin, S., Valipour, M.S., Rashidi, S., Convetcion-radiation heat transfer in solar heat exchangers filled with a porous medium: homotopy perturbation method versus numerical analysis. *Renewable Energy*, 74, pp. 448-455. doi: 10.1016/j.renene.2014.08.044.

[7] Kametani, Y., Fukagata, K., Orlu, R., Schlatter, P., 2015. Effect of uniform blowing/suction in a turbulent boundary layer at moderate Reynolds number. *International Journal of Heat and Fluid Flow*, 55, pp. 132-142. doi: 10.1016/ijheatfluidflow.2015.05.019.

[8] Chandra Sekhar, B., Vijay Kumar P., Veera Krishna M., 2023. Changeable heat and mass transport of unsteady MHD convective flow past an infinite vertical porous plate. *Journal of Heat and Mass Transfer Research*, 10 (2), pp. 207-222. doi: 10.22075/JHMTR.2023.31618.1469.

[9] Akinbo B.J., Olajuwon B.I., 2022. Stagnation-point flow of a Walters' B fluid towards a vertical stretching surface embedded in a porous medium with elastic-deformation and chemical reaction. *Journal of Heat and Mass Transfer Research,*9 (1), pp. 27-38. doi: 10.22075/JHMTR.2022.21722.1313.

[10] Aly A., Chamkha A.J., Raizah Z.A., 2020. Radiation and chemical reaction effects on unsteady coupled heat and mass transfer by free convection from a vertical plate embedded in a porous medium. *Journal of Heat and Mass Transfer Research*, 7 (2), pp. 95-103. doi: 10.22075/JHMTR.2019.10763.1149.

[11] Umavathi, J.C., Chamkha, A.J., Mateen, A., Al-Mudhaf, A., 2009. Unsteady oscillatory flow and heat transfer in a horizontal composite porous medium channel. *Non-linear Analysis: Modelling and Control*, 14(3), pp. 379-415. doi: 10.15388/NA.2009.14.3.14503.

[12] Deghan M., Valipour, M.S., Keshmiri, A., Saedodin, S., Shokri, N., 2016. On the thermally developing forced convection through a porous media under the local thermal non-equilibrium condition: an analytical study. *International Journal of Heat and Mass Transfer*, 92, pp. 815-823. doi: 10.1016/j.ijheatmasstransfer.2015.08.091.

[13] Deghan, M,Valipour, M.S., Saedodin, S., 2015. Temperature-dependent conductivity in forced convection of heat exchangers filled with porous media: a perturbation solution. *Energy Conversion and Management*, 92, pp.

259-266. doi: 10.1016/j.enconman.2014.12.011.

[14] Deghan, M., Valipour, M.S., Saedodin, S., Mahmoudi, Y., 2016. Investigation of forced convection through entrance region of a porous filled micro channel: an analytical study based on scale analysis. *Applied Thermal Engineering*, 99, pp. 446-454. doi: 10.1016/j.applthermaleng.2015.12.086.

[15] Chakravarty, A., Datta, P., Ghosh, K., Sen, S., Mukhopadhyay, A., 2018. Mixed convection heat transfer in an enclosure containing a heat generating porous bed under the influence of bottom injection. *International Journal of Heat and Mass Transfer*, 117, pp. 645-657. doi: 10.1016/j.ijheatmasstransfer.2017.10.046.

[16] Sheremet, M.A., Rosca, N.C., Rosca, A.V., Pop, I., 2018. Mixed convection heat transfer in a square porous cavity filled with a nanofluid with suction/injection effect. *Computers and Mathematics with Applications*, 76 (11-12), pp. 2665-2677. doi: 10.1016/j.camwa.2018.08.069.

[17] Gupta, A.S., Misra, J.C., Reza, M., 2003. Effects of suction or blowing on the velocity and temperature distribution in the flow past a porous flat plate of a power-law fluid. *Fluid Dynamics Research*, 32 (6), pp. 283-294. doi: 10.1016/S0169-5983(03)00068-6.

[18] Radnia, H., Nazar, A.R.S., 2017. Temperature profile of a power-law fluid flowing over a moving wall with arbitrary injection/suction and internal heat generation/absorption. *Journal of Heat and Mass Transfer Research*, 4 (1), pp. 53-64. doi:10.22075/JHMTR.20175.519.

[19] Mustapha, El., Hamma., Ilham A., Mohammed, T., Ahmed, R., Kamal, G., 2023. Analysis of MHD thermosolutal convection in a porous cylindrical cavity filled with a Casson nano fluid, considering Soret and Dufour effects. *Journal of Heat and Mass Transfer Research*, 10 (2), pp. 197-206. doi: 10.22075/JHMTR.2023.30532.1439.

[20] Madhy, A., 2016. Unsteady MHD slip flow of a non-Newtonian Casson fluid due to a stretching sheet with suction or blowing effect. *Journal of Applied Fluid Mechanics*, 9 (2), pp. 785-793. doi: 10.18869/ACADPUB.JAFM.68.225.24687.

[21] Dash, G.C., Ojha, K.L., 2018. Viscoelastic hydromagnetic flow between two porous parallel plates in the presence of sinusoidal pressure gradient. *Alexandria Engineering Journal*, 57 (4), pp. 3463-3471. doi: 10.1016/j.aej.2017.12.011.

[22] Khan, M.B., Sasmal, C., 2023. Electro-elastic instability in electroosmotic flows of viscoelastic fluids through a model porous system. *European Journal of Mechanics – B/Fluids*, 97, pp. 173-186. doi: 10.1016/j.euromechflu.2022.10.004.

[23] Padma Devi, M., Srinivas, S., 2023.Two layered immiscible flow of viscoelastic liquid in a vertical porous channel with Hall current, thermal radiation and chemical reaction. *International Communications in Heat and Mass Transfer*, 142, p.106612. doi: 10.1016/j.icheatmasstransfer.2023.106612.

[24] Ariel, P.D. 2002. On exact solutions of flow problems of a second grade fluid through two parallel porous walls. *International Journal of Engineering Science*, 40 (8), pp. 913-941. doi: 10.1016/S0020-7225(01)00073-8.

[25] Akbarzadeh, P., 2016. Pulsatile magnetohydrodynamic blood flows through porous blood vessels using a third-grade non-Newtonian fluid model. *Computer Methods and Programs in Biomedicine*, 126, pp.3-19. doi: 10.1016/j.cmpb.2015.12.016.

[26] Hassan, A.R., Salawu, S.O., 2019. Analysis of buoyancy driven flow of a reactive heat generating third grade fluid in a parallel channel having convective boundary conditions. *SN.Applied Sci*ences, 1, 919. doi: 10.1007/s42452-019-0864-y.

[27] Hayat, T., Ahmed, N., Sajid, M., 2008. Analytic solution for MHD third order fluid in a porous channel. *Journal of Computational and Applied Mathematics*, 214 (2), pp. 572-582. doi: 10.1016/j.cam.2007.03.013.

[28] Adesanya S.O., Falade J.A., 2015. Hydromagnetic third grade fluid flow through a channel filled with porous medium. *Alexandria Engineering Journal*, 54(3), pp. 615-622. doi: 10.1016/j.aej.2015.05.014.

[29] Hatami, M., Ganji, D.D., 2014. Thermal and flow analysis of micro channel heat sink (MCHS) cooled by Cu-water nano fluid by porous media approach and least square method. *Energy Conversion and Management*, 78, pp. 347-358. doi: 10.1016/j.enconman.2013.10.063.